of the lighter cells which have burst (Figure 2 *e*). There is some deformation of the organelles in the cytoplasm, like the lipid droplet here. This can be attributed only to the muscular contraction of the alveoli by the myoepithelial cells. The darker cell organelles show less deformation, but they also indicate high cellular activity. Most nuclei show chromatin margination and a fibrous nuclear lamina (which may structurally help retaining nuclear integrity as the cell is subjected to mechanical force). The SER in the dark cells shows, in places, a parallel array or honeycomb structure (Figure 2 *f, g*), a feature which has been reported in cells undergoing hypertrophy[8]. The bursting of the plasma membrane does not indicate necrosis, as the nuclei have not become swollen or pyknotic, nor is there swelling of mitochondria which tend to become pyknotic. In some Golgi vesicles (and cytoplasm), multivesicular bodies are seen, as also lipofuscin granules which are indicative of autophagy[7]. Dihydrotestosterone, a degradation product of testosterone and a more potent androgen, has also been reported in musth secretions[4]. Some alveoli, where the cells remained inactive, were also noticed. The cells here did not take up electron stain and just a few nuclei got stained. Additional evidence for the above discussion is presented in Figure 3.

The features noticed suggest the following. For steroid production, the cells go into a hypertrophic state with increase in numbers and tubular cristae of mitochondria, concomitant increase in SER and Golgi bodies with many secretory vacuoles, microvilli and changes in nuclei. Secretory products build up and they are sent out. Autophagy of lipids also takes place. When the limit of steroid synthesis is reached, microvilli disappear, the plasma membrane breaks and cellular debris enters the lumen along with the testosterone and dihydrotestosterone produced, as a result of the contractile forces exerted by the myoepithelial cells. This needs to be compared with mammary gland development, where epithelial stem cells in alveoli differentiate suitably for the production of milk protein and fat. It is interesting that in the temporal gland of the elephant they develop into androgen-secreting cells. The role of mitchondria and its changes during the production of androgen offers scope for biochemical investigations. It has been reported that younger males have in their musth secretion compounds which are honey-smelling (termed *moda* musth), which is tolerated by the older elephants and which in ancient Sanskrit literature is described as capable of attracting honey bees[9]. The present study also invokes the need to compare Asian musth gland ultrastructure with the younger male of the Asian elephant in moda musth, as also the male and female African elephants during normal temporal gland secretion activity and in musth. Along with the physiology involved, these studies can help in reducing human–elephant conflicts arising out of musth activity and perhaps even pave the way for a better understanding and treatment of endocrine diseases.

1. Rasmussen, L. E. L., Hess, D. L. and Haight, J. D., Chemical analysis of temporal gland secretions from an Asian bull elephant during musth. *J. Chem. Ecol.*, 1990, **16**, 2167–2181.
2. Das, A. K., *Flora and Fauna in Mughal Art* (ed. Som Prakash Verma), Marg Publications, Mumbai, 1999, p. 49.
3. Poole, J. H. and Moss, C., Musth in the African elephant *Loxodonta africana*. *Nature*, 1981, **292**, 830–831.
4. Rasmussen, L. E. L., Buss, I. O., Hess, D. L. and Schmidt, M. J., Testosterone and dihydrotestosterone in elephant serum and temporal gland secretion. *Biol. Reprod.*, 1984, **30**, 352–362.
5. Slotow, R., van Dyke, G., Poole, J., Page, B. and Klocke, A., Older bull elephants control young males. *Nature*, 2000, **408**, 425–426.
6. Estes, J. A. and Buss, I. O., Microanatomical structure and development of the African elephant's temporal gland. *Mammalia*, 1976, **40**, 429–436.
7. Cross, P. C. and Mercer, K. L., *Cell and Tissue Ultrastructure*, W.H. Freeman and Co., New York, 1993.
8. Ghadially, F. N., *Ultrastructural Pathology of the Cell and Matrix*, Butterworths, New York, 1987, 3rd edn.
9. Rasmussen, L. E. L., Riddle, H. S. and Krishnamurthy, V., Mellifluous matures to malodorous in musth. *Nature*, 2002, **415**, 975–976.

ACKNOWLEDGEMENTS. We thank Dr S. Paulraj, the then Wildlife Warden, Mudumalai Wildlife Sanctuary, his staff Mr P. R. Mani, Mr Babu and the mahouts, and Dr Shanmughasundaram, Forest veterinarian for their cooperation and help. We also thank Dr T. Ramasami, Director, Central Leather Research Institute, for use of facilities.

Received 17 June 2003; accepted 30 August 2003

Constructing 3D phylogenetic trees

M. Milner[†], Vidya Patwardhan[#], Ahron Bansode[*], S. A. Nevagi[†], Sucheta Kulkarni[##], Rohinton Kamakaka[††] and Sohan P. Modak[†,‡,]**

[†]Department of Zoology, Karnatak University, Dharwad 580 003, India
[#]Agharkar Research Institute, Pune 411 004, India
[*]Ahmednagar College, Ahmednagar 414 001, India
[##]Department of Molecular Cardiology, Lerner Research Institute, Cleveland, Ohio 44195, USA
[††]National Institute of Child Health and Human Development, Building 18T, Bethesda, MD 20892, USA
[‡]Open Vision, 759/75, Deccan Gymkhana, Pune 411 004, India

Lens crystallins are highly conserved, tissue-specific proteins. Crystallins from eight vertebrates were compared on the basis of their isoelectric points, molecular weights and immuno-crossreactivity against polyclonal antibodies using 3D plots, to estimate 'star' and 'network' Euclidian distances between species. The phylogenetic trees obtained were tested by bootstrap and fixed in the 3D space by multidimensional scaling and a new sequential positioning method. 3D trees using 'network' distances give the best fits.

THE vertebrate eye lens contains tissue-specific (α, β and γ or δ) crystallins, which have been compared[1–22] for

**For correspondence. (e-mail: spmodak@rediffmail.com)

phylogenetic closeness based on their immuno-cross-reactivity. At present, phylogenetic trees are constructed based on a single parameter or trait, using unweighted pairs grouping method[23–25]. Such trees are two-dimensional and with corrections for the timescale[1,4,15–17,26–30]. They offer solutions which differ depending on the parameter. From our database (S. P. Modak and M. Milner, 2002, unpublished) on isoelectric points (pI), molecular weight (MW) and immuno-crossreactivity (IC) of vertebrate crystallins to eight antibodies, we describe the construction of 3D phylogenetic trees by multidimensional scaling or a novel sequential positioning of 3D distances in combination with unweighted pairs grouping.

The database (S. P. Modak and M. Milner, 2002, unpublished) of over 150 vertebrate species[1,8,16,17,25] categorizes vertebrate lens crystallins by MW in SDS–PAGE, by pI in isoelectrofocusing gels (IEF–PAGE), and IC against polyclonal antibodies to crystallins from eight different vertebrates[1,8,15,17,25]. We compared crystallins from shark (*Scoliodon sorrakowah*, order Lamniformes, subclass Chondropterygii, class Pisces), pomfret (*Pampus argenteus*, order Perciformes, subclass Teleostei, class Pisces), frog (*Rana tigerina*, order Anura, class Amphibia), garden lizard (*Calotes versicolour*, order Lacertilia, class Reptilia), chick (*Gallus domesticus*, order Galliformes, class Aves), and three mammals, namely, mouse (*Mus musculus*, order Rodentia, class Mammalia), fruit bat (*Rousettus leschenaulti*, suborder Megachiroptera, order Chiroptera, class Mammalia) and Megaderma (*Megaderma lyra*, suborder Microchiroptera, order Chiroptera, class Mammalia) to obtain the similarity coefficient[31] [S] based on the fraction of number of bands of MW or pI and precipitin lines in IC common to any two species, using the equation [$S = Z/(X + Y–Z)$], where S is the fraction of shared bands, X is the total number of bands in species A, Y is the total number of bands in species B and Z is the number of bands common to species A and B. We then estimate (Table 1) the number of changes per protein [P value] as $P = –[\ln S]/N$, where N is 3 for α, β and γ or δcrystallins, and $\ln S$ is the natural logarithm of the S value. Using '3D Studio VIZ' Release 3, we plot in 3D, P values for IC precipitin lines (x axis), IEF classes (y axis) and MW classes (z axis) of crystallins. In these plots, the P values for MW and pI are the same, while those for IC are relative to any one species with its homologous reaction and positioned at 0, 0, 0 from where we estimate three-dimensional or Euclidian distances to each of the seven remaining species, using the equation $D = \sqrt{\{(x1 - x2)^2 + (y1 - y2)^2 + (z1 - z2)^2\}}$. These are termed as 'star' distances. Here, D is the distance between the species $P1$ located at $x1$, $y1$, $z1$ giving a homologous IC, and the species $P2$ located at $x1$, $y2$ and $z2$, showing heterologous IC, and so on for species P3 to P8. When compared bi-directionally within a pair, 3D distances may differ because of the number of precipitin lines in homologous IC. For example, in homologous IC, shark forms five precipitin lines, while pomfret gives nine, which may affect their relative bi-directional 'star' or

Table 1. Estimated number of changes per protein (P value) in crystallins

	Shark			Pomfret			Frog			*Calotes*		
	IC	pI	MW	IC	pI	MW	IC	pI	MW	IC	pI	MW
Shark	0.000	0.000	0.000	0.305	0.414	0.536	0.187	0.740	0.693	0.768	1.277	0.462
Pomfret	0.597	0.414	0.536	0.000	0.000	0.000	0.337	0.617	0.478	0.462	0.590	0.519
Frog	0.501	0.740	0.693	0.337	0.617	0.478	0.000	0.000	0.000	0.366	0.489	0.672
Calotes	0.501	1.277	0.462	0.624	0.590	0.519	0.231	0.489	0.672	0.000	0.000	0.000
Chick	0.282	0.903	0.418	0.597	0.774	0.401	0.327	0.497	0.366	0.327	0.300	0.513
Mouse	0.536	0.693	0.536	0.489	0.511	0.568	0.270	0.544	0.462	0.401	0.672	0.513
Rousettus	0.327	0.732	0.649	0.624	0.523	0.649	0.366	0.613	0.536	0.366	0.641	0.462
Megaderma	0.501	0.672	0.536	0.880	0.491	0.568	–	0.568	0.462	–	0.649	0.513
	Chick			Mouse			*Rousettus*			*Megaderma*		
	IC	pI	MW	IC	pI	MW	IC	pI	MW	IC	pI	MW
Shark	1.000	0.903	0.418	0.231	0.693	0.536	0.768	0.732	0.649	0.501	0.672	0.536
Pomfret	1.000	0.774	0.401	0.170	0.511	0.568	0.462	0.523	0.649	0.624	0.491	0.568
Frog	0.327	0.497	0.366	0.270	0.544	0.462	0.536	0.613	0.536	0.536	0.568	0.462
Calotes	0.327	0.300	0.513	0.568	0.672	0.513	0.536	0.641	0.462	0.536	0.649	0.513
Chick	0.000	0.000	0.000	0.366	0.679	0.578	0.501	0.649	0.693	0.501	0.657	0.578
Mouse	0.799	0.679	0.578	0.000	0.000	0.000	0.157	0.049	0.074	0.157	0.036	0.000
Rousettus	0.501	0.649	0.693	0.051	0.049	0.074	0.000	0.000	0.000	0.000	0.013	0.074
Megaderma	–	0.657	0.578	0.157	0.036	0.000	0.231	0.013	0.074	0.000	0.000	0.000

IC, Immunocrossreactive precipitin lines; pI, Isoelectric classes; MW, Molecular weight classes.

Table 2. 'Star' distance among individual species

Distance	Shark	Pomfret	Frog	*Calotes*	Chick	Mouse	*Rousettus*	*Megaderma*
Shark	0.00							
Pomfret	0.82 ± 0.11	0.00						
Frog	1.08 ± 0.07	0.85 ± 0.00	0.00					
Calotes	1.50 ± 0.08	0.96 ± 0.06	0.89 ± 0.03	0.00				
Chick	1.22 ± 0.27	1.19 ± 0.19	0.70 ± 0.00	0.68 ± 0.00	0.00			
Mouse	0.97 ± 0.09	0.85 ± 0.09	0.76 ± 0.00	0.98 ± 0.06	1.08 ± 0.17	0.00		
Rousettus	1.14 ± 0.15	1.00 ± 0.06	0.93 ± 0.06	0.91 ± 0.06	1.07 ± 0.00	0.14 ± 0.05	0.00	
Megaderma	1.00 ± 0.00	1.07 ± 0.13	0.82 ± 0.12	0.91 ± 0.11	0.94 ± 0.09	0.16 ± 0.00	0.16 ± 0.12	0.00

±Standard deviation of the mean.

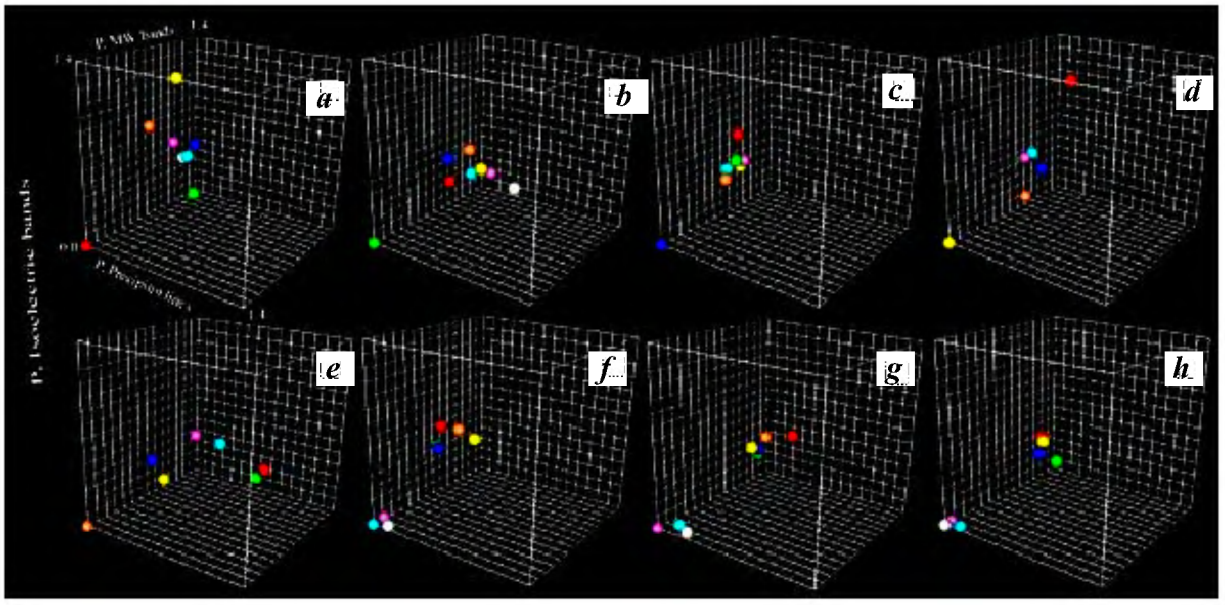

Figure 1. Three-dimensional phylogenetic relationships among eight vertebrate lens crystallins based on their pI, MW and IC with polyclonal antibodies against crystallins from (***a***) Red, Shark, (***b***) Green, Pomfret, (***c***) Deep blue, Frog, (***d***) Yellow, *Calotes*, (***e***) Orange, Chick, (***f***) Light blue, Mouse, (***g***) Purple, *Rousettus* and (***h***) White, *Megaderma*. All homologous reacting species are placed at the origin (0, 0, 0).

Euclidian distances, so that the star distance between shark-*Ab* to pomfret-*Ag* is 0.9032, while it is 0.7432 in the opposite direction (Table 2).

We have also determined the Euclidian 'network' distances among seven reacting heterologous antigens in each plot in Figure 1, which give seven measurements for each pair of antigen–antibody IC (Table 3).

We have used the unweighted pairs grouping method of Fitch and Margoliash[23], using the software MEGA (Molecular Evolutionary Genetics Analysis, version 1.2, The Pennsylvania State University) to draw a phylogenetic tree based on *P* values for individual traits of crystallins, namely pI, MW and IC, as well as those based on Euclidian distances in multi-parametric analyses. The latter were then subjected to bootstrap to assess the confidence limits[32,33].

From the mean and the standard deviation of the observed distances, two normal, random (U_1 and U_2) numbers with the same mean were generated using Box and Muller method[34]. The values of U_1 and U_2 were between 0 to 1 and the values of two variables X and Y were calculated using the formulae $X = (-2\log U_1)\sin(2\pi U_2)$ and $Y = (-2\log U_1)\cos(2\pi U_2)$. The bootstrap sample distances were calculated by the equation $X_1 = sX + m$ and $Y_1 = sY + m$, where s is the standard deviation, m is the mean, and X_1 and Y_1 are the bootstrap distances. With this method, 1000 distances (500 pairs) were generated and analysed for unweighted pairs grouping method using the software MEGA. The trees were compared for the species sequence and stem-fork relationships as well as class-specific clustering. With the maximal similarity designated as 1.0, the normal approximation to binomial probability is used to calculate the confidence limits for observing trees similar to the mean. The bootstrap confidence limits were calculated using the equation $CL = P \pm 1.96\sigma$, where CL is the confidence limit, P is the

Table 3. 'Network' distance among individual species

Distance	Shark	Pomfret	Frog	*Calotes*	Chick	Mouse	*Rousettus*	*Megaderma*
Shark	0.00							
Pomfret	0.39 ± 0.26	0.00						
Frog	0.50 ± 0.39	0.38 ± 0.30	0.00					
Calotes	0.54 ± 0.52	0.53 ± 0.33	0.36 ± 0.29	0.00				
Chick	0.55 ± 0.50	0.43 ± 0.42	0.31 ± 0.19	0.31 ± 0.20	0.00			
Mouse	0.64 ± 0.35	0.46 ± 0.34	0.51 ± 0.30	0.61 ± 0.32	0.57 ± 0.35	0.00		
Rousettus	0.71 ± 0.34	0.54 ± 0.36	0.53 ± 0.31	0.60 ± 0.35	0.59 ± 0.36	0.18 ± 0.08	0.00	
Megaderma	0.67 ± 0.31	0.45 ± 0.38	0.52 ± 0.30	0.60 ± 0.31	0.58 ± 0.35	0.11 ± 0.14	0.13 ± 0.08	0.00

±Standard deviation of the mean.

Table 4. Three-dimensional distance among individual species from 'star' MDS plot

Distance	Shark	Pomfret	Frog	*Calotes*	Chick	Mouse	*Rousettus*	*Megaderma*
Shark	0.00							
Pomfret	0.83 ± 0.01	0.00						
Frog	0.89 ± 0.19	0.83 ± 0.02	0.00					
Calotes	1.52 ± 0.02	0.96 ± 0.00	0.88 ± 0.01	0.00				
Chick	1.45 ± 0.22	1.23 ± 0.03	0.58 ± 0.12	0.68 ± 0.00	0.00			
Mouse	0.94 ± 0.03	0.88 ± 0.04	0.83 ± 0.06	0.93 ± 0.04	1.03 ± 0.05	0.00		
Rousettus	1.09 ± 0.05	0.99 ± 0.01	0.93 ± 0.00	0.92 ± 0.01	1.05 ± 0.02	0.15 ± 0.01	0.00	
Megaderma	1.03 ± 0.04	1.01 ± 0.06	0.82 ± 0.00	0.93 ± 0.02	0.95 ± 0.01	0.16 ± 0.00	0.16 ± 0.00	0.00

±Standard error of the mean.

Table 5. Three-dimensional distance among individual species from 'star' SP plot

Distance	Shark	Pomfret	Frog	*Calotes*	Chick	Mouse	*Rousettus*	*Megaderma*
Shark	0.00							
Pomfret	0.82 ± 0.00	0.00						
Frog	0.64 ± 0.44	0.58 ± 0.27	0.00					
Calotes	1.50 ± 0.00	1.11 ± 0.15	0.94 ± 0.05	0.00				
Chick	1.22 ± 0.00	1.19 ± 0.00	0.70 ± 0.00	0.68 ± 0.00	0.00			
Mouse	0.97 ± 0.00	0.91 ± 0.07	0.86 ± 0.10	0.98 ± 0.00	1.08 ± 0.00	0.00		
Rousettus	1.10 ± 0.04	1.00 ± 0.00	0.94 ± 0.00	0.91 ± 0.00	1.07 ± 0.00	0.14 ± 0.00	0.00	
Megaderma	0.99 ± 0.00	0.96 ± 0.11	0.81 ± 0.01	0.87 ± 0.03	0.94 ± 0.00	0.16 ± 0.00	0.16 ± 0.00	0.00

±Standard error of the mean.

probability of observing trees similar to mean distances tree and σ is calculated using the formula $\sigma = \sqrt{(P(1-P)/n)}$, for n samples.

The mean 'star' and/or 'network' distances were subjected to MDS (Multidimensional Scaling, version 1.13, http://www.let.rug.nl/~kleiweg/levenshtein) and the positions of all species were plotted in 3D space from X, Y, Z coordinates in the output. From these plots, Euclidian distances among all species were re-estimated (Tables 4 and 5); the per cent error = $(dd/ad) \times 100$, where dd is the sum of variation in actual and fixed distances, and ad is the sum of actual distances. Phylogenetic trees were also constructed from the Euclidian distances in MDS as before, and the homology network was generated by sequentially joining each stem to the midpoint of the fork.

We have developed and programmed in JAVA a sequential positioning (SP) algorithm (Milner and Modak, 2003, unpublished), to fix the positions of species in 3D space. Here, beginning with a species placed at the origin, the second species was placed on the X-axis at a distance equal to that calculated from the Figure 1, and the third species was placed in the XY plane. From the 4th species onwards they were plotted in the XYZ space, roughly at the calculated distances. For the eight species in question, the average bi-directional 3D distances estimated between two species from IC data were used. It should be noted that species might fall in different quadrants. Again, the Euclidian distances among all species were estimated (Tables 6 and 7) along with percent error as before. The method is applied to 'star' and 'network' distances separately. Again, phylogenetic trees were con-

Table 6. Three-dimensional distance among individual species from 'network' MDS plot

Distance	Shark	Pomfret	Frog	*Calotes*	Chick	Mouse	*Rousettus*	*Megaderma*
Shark	0.00							
Pomfret	0.36 ± 0.03	0.00						
Frog	0.56 ± 0.05	0.33 ± 0.05	0.00					
Calotes	0.52 ± 0.02	0.56 ± 0.03	0.43 ± 0.06	0.00				
Chick	0.53 ± 0.02	0.46 ± 0.03	0.23 ± 0.08	0.26 ± 0.05	0.00			
Mouse	0.62 ± 0.02	0.44 ± 0.02	0.51 ± 0.01	0.58 ± 0.03	0.62 ± 0.05	0.00		
Rousettus	0.74 ± 0.03	0.55 ± 0.01	0.52 ± 0.01	0.57 ± 0.04	0.61 ± 0.02	0.18 ± 0.00	0.00	
Megaderma	0.68 ± 0.01	0.45 ± 0.01	0.48 ± 0.04	0.60 ± 0.00	0.61 ± 0.03	0.10 ± 0.00	0.13 ± 0.00	0.00

±Standard error of the mean.

Table 7. Three-dimensional distance among individual species from 'network' SP plot

Distance	Shark	Pomfret	Frog	*Calotes*	Chick	Mouse	*Rousettus*	*Megaderma*
Shark	0.00							
Pomfret	0.39 ± 0.00	0.00						
Frog	0.55 ± 0.04	0.37 ± 0.01	0.00					
Calotes	0.53 ± 0.02	0.58 ± 0.05	0.36 ± 0.00	0.00				
Chick	0.50 ± 0.05	0.39 ± 0.04	0.10 ± 0.21	0.31 ± 0.00	0.00			
Mouse	0.64 ± 0.00	0.46 ± 0.00	0.57 ± 0.07	0.62 ± 0.01	0.62 ± 0.05	0.00		
Rousettus	0.72 ± 0.00	0.54 ± 0.00	0.53 ± 0.00	0.55 ± 0.05	0.58 ± 0.00	0.18 ± 0.00	0.00	
Megaderma	0.67 ± 0.01	0.45 ± 0.00	0.51 ± 0.01	0.60 ± 0.00	0.57 ± 0.01	0.11 ± 0.00	0.13 ± 0.00	0.00

±Standard error of the mean.

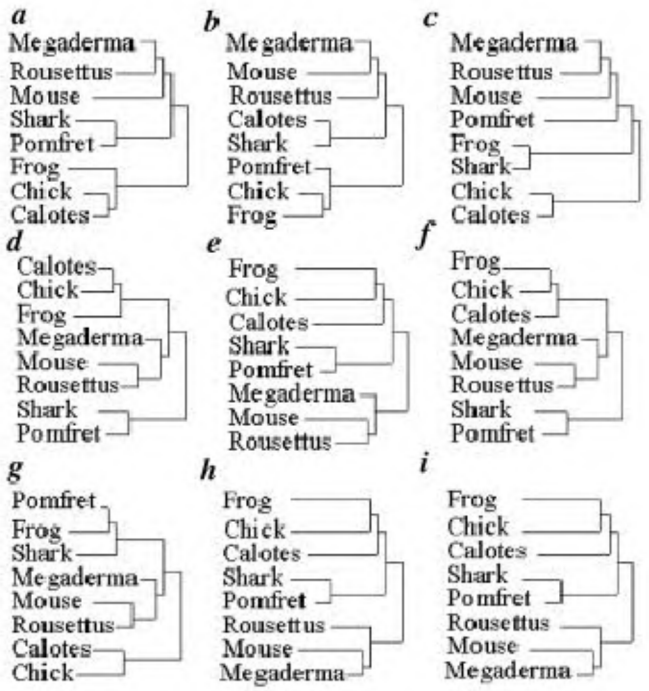

Figure 2. Phylogenetic relationship by unweighted pairs grouping[23] among eight species based on (*a*) Isoelectric focusing [pI], (*b*) Molecular weight [MW], (*c*) Immuno-crossreactivity [IC], (*d*) 3D star distances, (*e*) 3D network distances, (*f*) Multidimensional scaling [MDS] of 3D star distance, (*g*) Sequential positioning [SP] of 3D-star distance, (*h*) MDS of 3D network distance and (*i*) SP of 3D network distance.

structed from the Euclidian distances in SP as before and represented in 3D plots as above.

This study uses pI, MW and IC as parameters describing homology of lens crystallins from two fishes, one amphibian, one reptile, one bird and three mammals[1,2,5,8,15–17]. We obtained the similarity index and *P* value[31] designating number changes per protein (Table 1) for independent comparison of three parameters for each species among eight vertebrates. These were plotted in 3D such that in each plot *P* values for MW, pI and homologous IC were positioned at the origin (0, 0, 0). We find (Figure 1 *a–h*) that mammals are clustered together irrespective of the antibody used. In contrast, fishes, on one hand, and chicks, frogs and lizards, on the other, form dispersed clusters. It is notable that when individual parameters are used, in the phylogenetic trees generated by the Fitch–Margoliash[23] method, the positions of lower vertebrates differ from each other (Figure 2 *a–c*), while from both 'star' and 'network' 3D coordinates, mammals and fishes retain discrete clusters, while frogs, lizards and chicks interchange their positions. Thus, similar to earlier findings[2], the present method shows that mouse (order Rodentia) and *R. leschenaulti* (suborder Megachiroptera) are very close and are immediately followed by *M. lyra* (suborder microchiroptera). Thus, the phylogenetic relationship differs significantly among eight vertebrates spanning all classes, depending on the parameter/character/trait, while showing the phylogenetic sequence and parsimony derived from multi-parametric analysis is closer to the known taxonomic positions and of much greater value. The present IC data based on the use of polyclonal antibody are made against total lens crystal-

lins which include three molecular classes (α, β and γor δ), each composed of two or more subunits, and a total of more than 15 polypeptide products of distinct genes. Therefore, a polyclonal antiserum actually offers the entire panel against detectable epitopes and is far more suitable than monoclonal antibodies which would otherwise require an exhaustive panel to account for crossreactivity with thousands of epitopes in multiple proteins. Such panels are neither available nor have they been used in a phylogenetic study. In any case, in the present study the IC data are based on precipitin lines formed by the target antigen against challenging antibody in immunoelectrophoresis wherein each protein class among α, β, and γor δcrystallins is represented by 1 to 4 lines depending on the species used. Thus, the IC data are representative of multiple traits; three based on crystallin class, or 15 or more based on polypeptide number.

From the plots (Figure 1), 'star' Euclidian (3D) distances between the species at the origin and the remaining seven were estimated, which gives two measurements for each pair (Table 2). The mean value was subjected to unweighted pairs grouping method[23] and the CL on the fits was assessed by bootstrap yielding a CL value for of 0.48 ± 0.09. When this procedural sequence is applied to 'network' distances (Table 3), the CL is estimated as 0.82 ± 0.07. We have also combined the 'star' and 'network' distances and the ensuing analysis gives the fits with a CL of 0.69 ± 0.09 (not shown). We conclude that

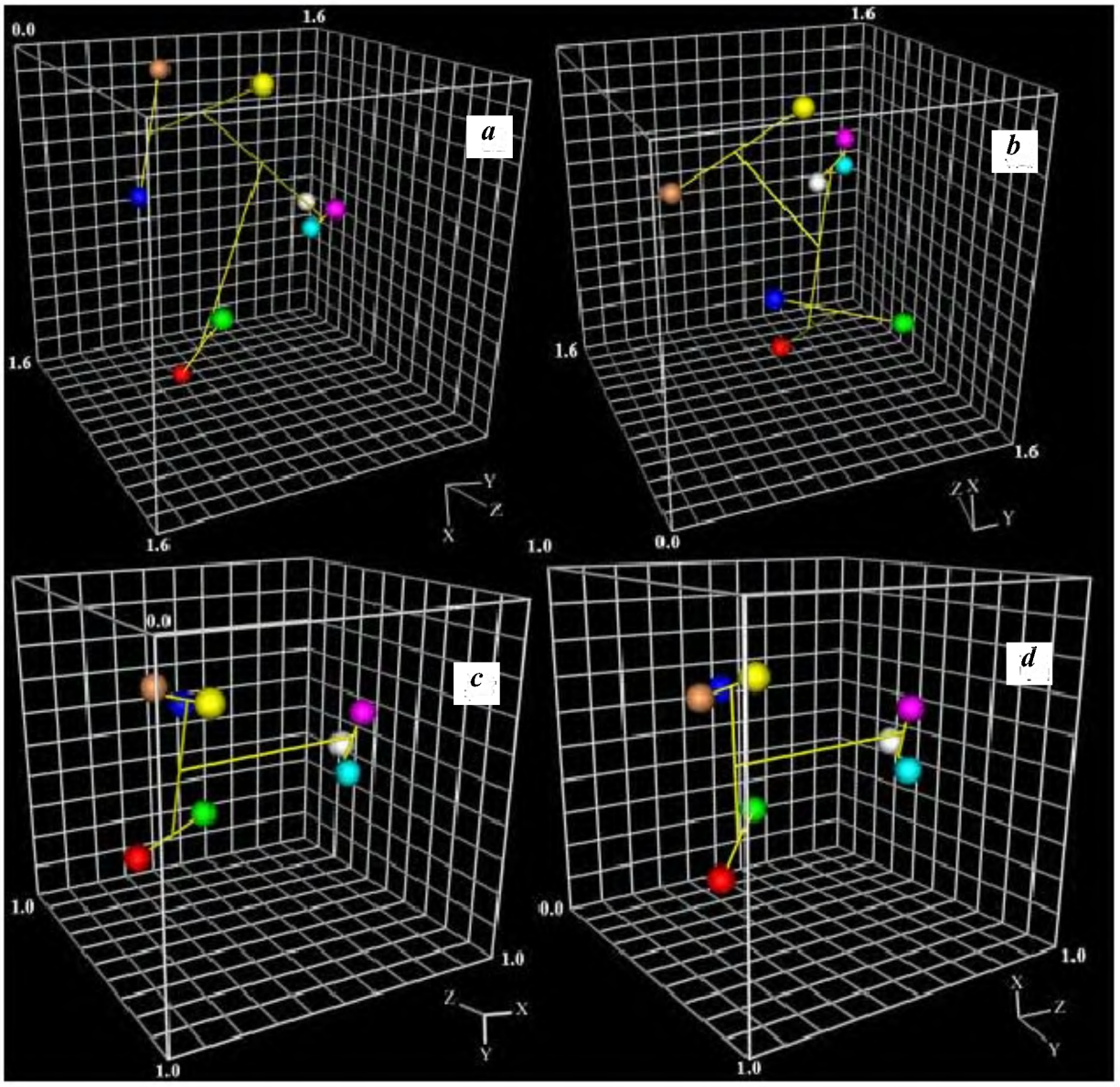

Figure 3. 3D phylogenetic trees of vertebrate crystallins by combining unweighted pairs grouping method with (***a***) Star-MDS, (***b***) Star-SP, (***c***) Network-MDS and (***d***) Network-SP. Note discrete clustered positions for mammals (***a–d***) and fishes (***a***, ***c***, ***d***). Red, Shark; Green, Pomfret; Deep blue, Frog, Yellow, *Calotes*; Orange, Chick; Light blue; Mouse, Purple, *Rousettus* and White, *Megaderma*.

phylogenetic trees using 'network' Euclidian distances from 3D plots give the best fits. In fact, when 3D distances are subjected to MDS followed by treatment with unweighted pairs grouping method[23], the resultant tree (Figure 2 *h*) is similar to that based on 'network' distances alone (Figure 2 *e*); in both cases Pisces, mammals and the remaining vertebrates form three distinct clusters. In any case, MDS plots using either 'star' or 'network' distances give an error bar between 4.4 and 5.7%. The phylogenetic relationship (Figure 2 *f*) from MDS (Figure 3 *a*) shows that the shark and pomfret together form the base of the stem, giving off a mammalian branch and another holding amphibians, Aves and reptiles. This relationship (Figure 2 *d*) differs significantly from those using unique parameters (Figure 2 *a–c*).

We have developed the SP method in which the 3D distances (Table 2) are used sequentially to position species relative to each other. Since mammals appear very close (Figure 2 *a–c*), we have tentatively fixed the positions of three mammals, and the best positioning fits of the remaining five species were computed and compared to actual distances (Tables 2 and 3). The one giving the least difference was designated as the 4th species. The same procedure is followed sequentially for positioning the rest of the species. From the coordinates based on 'star' distances in SP, a 3D plot was drawn (Figure 3 *b*) and the corresponding Euclidian distances among eight species (Tables 4 and 5) were processed for unweighted pairs grouping method giving a phylogenetic tree (Figure 2 *h*). We see the trees obtained from 'star' data (Figure 2 *d*); star MDS (Figure 2 *f*) and SP (Figure 2 *h*) are substantially different from one another. *Calotes* is closest to the chick, while mammals form a separate cluster. The 3D phylogenetic tree (Figure 3 *b*) obtained by combining SP with the Fitch–Margoliash protocol[23] differs from that obtained with MDS (Figure 3 *a*). When MDS and SP 3D plots from 'network' distances (Table 3) are combined with unweighted pairs grouping, we find both in agreement. Thus, at present, both models appear reasonable. We have also examined the 3D positioning of the eight species on the basis of the Mahalanobis distance which is a squared distance between two points in a multidimensional space, from the equation $r^2 = (x - m_x)' c_x^{-1} (x - m_x)$, where r is the Mahalanobis distance, x the input vector, m_x the mean vector and C_x is the covariance matrix for x. Mahalanobis distances calculated for 'star' and 'network' distances (not shown) from Figure 1 were processed for MDS and SP. The phylogenetic trees constructed from 3D distances re-estimated from 3D coordinates of MDS/SP show that the error was 5% for Euclidean distances and between 30 and 50% for Mahalanobis distances. Thus, the present data do not fall under Mahalanobis coordinates, but the fits should be compared using Euclidean and Mahalanobis distances.

In this communication we have used only eight representatives of the subphylum vertebrata that allow distinction among classes, subclasses in general and up to suborder in mammals. Clearly, a phylogenetic tree based on multiple parameters is closer to reality than that based on a single trait/character/property.

Recently, we have applied the method to generate a 3D phylogenetic tree for β-globin from 12 species using amino acid sequence, cDNA nucleotide sequence and the globin gene nucleotide sequence (between proximal 5′ TATA box and the 3′ polyadenylation signal). We find that the multiparametric tree gives a better understanding of the evolutionary closeness compared to the individual traits.

In conclusion, high-resolution 3D phylogenetic trees can be constructed using parameters such as pI, MW and IC or any other relevant attribute/s of a character/trait to give discrete phylogenetic relationships based on multiple parameters/traits.

1. Bansode, A. J., Evolutionary relationship in Chiroptera: Biochemical analysis. Ph D thesis, University of Poona, Pune, 1985.
2. Brahma, S. K. and Van Doorenmaalen, W. J., Study of the soluble lens proteins from different amphibian species, *Exp. Eye Res.*, 1969, **8**, 168–171.
3. Clayton, R. M. Comparative aspects of lens protein. In *The Eye* (eds Davson, H. and Graham, Jr. L. T.), Associated Press, New York, 1974, vol. 5, pp. 399–494.
4. Day, T. H., Variations in the lens proteins among species of rodents. *Comp. Biochem. Physiol.* 1972, **B43**, 1019–1027.
5. De Jong, W. W., Gleaves, J. T. and Boulter, D., Evolutionary changes of α-crystallin and the phylogeny of mammalian orders. *J. Mol. Evol.*, 1977, **10**, 123–135.
6. Gysele, M., Immunoelectrophoresis of avian lens proteins. *Experientia*, 1964, **20**, 145–146.
7. Halbert, S. P., Manski, W. and Auerbach, T., Lens antigens in relation to evolution. In *Structure of the Eye* (ed. Smelser, G. K.), Academic Press, New York, 1961, pp. 249–258.
8. Kulkarni, S. N., Homology of Amphibian lens crystallins, M Phil dissertation, University of Poona, 1985, pp. 1–36.
9. Maisel, H. and Goodman, M., The ontogeny and specifity of human lens proteins. *Invest. Ophthalmol.*, **72**, 829–831.
10. Manski, W., Halbert, S. P. and Auerbach, T. P., Immunochemical analysis of the phylogeny of lens proteins. In *Taxonomic Biochemistry and Serology* (ed. Leone, C. A.), Ronald Press, New York, 1964, pp. 545–554.
11. Manski, W., Halbert, S. P. and Aurebachal-Pascal, T., On the use of antigenic relationships among species for the study of molecular evolution – III. The lens proteins of the late Actinopterygii. *Int. Arch. Allergy Appl. Immunol.*, 1967, **31**, 529–545.
12. Manski, W., Halbert, S. P., Aurebach-Pascal, T. and Janiver, P., On the use of antigenic relationships among species for the study of molecular evolution – I. The lens of the Agnatha and Chondrichthyes. *Int. Arch. Allergy Appl. Immunol.*, 1976, **31**, 38–56.
13. McDevitt, D. S. and Collier, C. R., The lens proteins of eastern north American salamanders, and their application to urodelan systematics. *Exp. Eye Res.*, 1976, **21**, 1–8.
14. Menezes, M. R. and Qasim, S. Z., Uses of electrophoresis and immuno-electrophoresis in taxonomic and pollution studies. *Proc. Indian Acad. Sci. (Anim. Sci.)*, 1984, **93**, 179–198.
15. Patwardhan, V. G., Jaswany, V. L., Pal, J. K. and Modak, S. P., Lens protein phylogeny: Immuno-crossreactivity of vertebrate lens antigens to antishark antibody. *Indian J. Biochem. Biophys.*, 1995, **32**, 21–31

16. Patwardhan, V. G. and Modak, S. P., Physicochemical characterization and phylogenetic comparison of fish lens proteins. *Indian J. Biochem. Biophys.* 1992, **29**, 498–507.
17. Patwardhan, V., Phylogeny of fish lens crystallins. Ph D thesis, University of Poona, 1992, pp. 1–101.
18. Puri, N., Augusteyn, R. C. Owen, E. A. and Siezen, R. J., Immunochemical properties of vertebrate α-crystallins. *Eur. J. Biochem.*, 1983, **134**, 321–326.
19. Smith, A. C., The electrophoretic characteristics of albacore blue fin tuna and kelp bass eye lens proteins. *Calif. Fish Game*, 1962, **48**, 199–201.
20. Swanborne, P. L., The method of simultaneous electrophoresis of antiserum and antigen (immunosmophoresis) applied to lens antigens. *Exp. Eye Res.*, **5**, 302–308.
21. Williams, L. H. and Piatigorsky, J., Comparative and evolutionary aspects of δ-crystallin in the vertebrate lens. *Eur. J. Biochem.*, 1979, **100**, 349–352.
22. Zigler, J. S. and Sidbury, Jr. J. B. A comparative study of β-crystallins from six mammals. *Comp. Biochem. Physiol.*, **53**, 349–355.
23. Fitch, W. M. and Margoliash, E., Construction of phylogenetic trees. *Science*, 1967, **155**, 279–284.
24. Goodman, M., Barnabas, J., Matsuda, G. and Moore, G. W., Molecular evolution in the descent of the man. *Nature*, 1971, **233**, 604–613.
25. Kamakaka, R. T., Homology of lens crystallins in Reptilia. M Phil dissertation, University of Poona, Pune, 1984, pp 1–24.
26. Barnabas, J., Goodman, M. and Moor, W., Evolution of hemoglobin in primates and other therian mammals. *Comp. Biochem. Physiol.*, 1971, **B39**, 455–482.
27. De Jong, W. W., Evolution of lens and crystallins. In *Molecular and Cellular Biology of the Eye Lens* (ed. Biomendal, H.), John Wiley, New York, 1981, Chapter 6, pp. 221–278.
28. Wilson, A. L., Carlson, S. S. and White, T. J., Biochemical evolution. *Annu. Rev. Biochem.*, 1977, **46**, 573–636.
29. Wright, C., *Biochemical and Immunochemical Taxonomy of Animals*. Academic Press, London, 1974.
30. Zuckerkandle, E. and Pauling, L., Evolutionary divergence and convergence in proteins. In *Evolving Genes and Proteins* (eds Bryson, V. and Vogel, H. J.), Academic Press, New York, 1965, pp. 97–166.
31. Brown, W. M., George, M. and Wilson, A. C., Rapid evolution of animal mitochondrial DNA. *Proc. Natl. Acad. Sci. USA*, 1979, **76**, 1967–1971.
32. Felsenstein, J., Confidence limits on phylogenies: An approach using the bootstrap. *Evolution*, 1985, **39**, 783–791.
33. Efron, B., Bootstrap methods: Another look at the jackknife. *Ann Stat.*, 1979, **7**, 1–26.
34. Box, G. E. P. and Muller, M. E., A note on the generation of random normal deviates. *Ann. Math. Stat.*, 1958, **28**, 610–611.
35. King, J. L. and Jukes, T. H., Non Darwinian evolution. *Science*, 1969, **164**, 788–795.

ACKNOWLEDGEMENTS. This work is part of the Ph D thesis of M. M. We thank Prof. S. K. Saidapur, Chairman, Department of Zoology, Karnatak University, Dharwad; Prof. N. V. Joshi, Centre for Ecological Sciences, Indian Institute of Science, Bangalore; Profs B. K. Kale, Sharayu Paranjape and M. B. Rajarshi, Department of Statistics, University of Pune, and Dr A. Saraph, Institute for Change Research, Goa, for critical comments and suggestions and Mr D. Prabhu for advise regarding computations.

Received 15 April 2003; revised accepted 23 July 2003

Physical and mineralogical evaluation of a brick sample from an ancient altar structure in Garhwal Himalayan region

J. M. Bhatnagar* and L. P. Singh

Clay Products Division, Central Building Research Institute, Roorkee 247 667, India

A brick sample from an ancient site at Purola situated in Garhwal Himalayan region was evaluated for its physical and mineralogical properties. The present investigations were aimed to assess the impact of environmental weathering on the building elements of the brick altar structure, which is said to be nearly 2000 years old. The finding reveals some interesting attributes of the burnt bricks used in the construction of the altar structure for performing certain rituals according to the vedic culture. Investigations based on X-ray diffraction and scanning electron microscope studies reveal that the deterioration of the brick body used in the construction was mainly due to physical and chemical factors. Results of laboratory findings are presented here.

AN ancient massive brick altar at Purola in Uttarkashi District in the Central Himalayan region was identified by a team of archaeologists in 1986–88 (ref. 1). The remains of the brick altar structure are situated on the left bank of river Kamal, a tributary of the major river Yamuna in the vicinity of the Indus Valley at Purola town (Figure 1). Earlier findings by geologists and archaeologists in the region, including remains of a temple structure at Lakhamandal, *syenachiti* at Jagatgram and Challis rock edict of the Ashoka regime are well documented[1–4]. Leaving aside the historical aspect of these ancient remains, the findings are vital to work out missing links in technological development in the field of building materials and technology, which took place during the past few thousand years in the Indus Valley. The first reference of brick–*istaka* appears in *Yajurveda*[5] for construction of altars of different geometrical shapes and sizes to perform specific rituals[4–7]. The excavated altar structure at Purola is in fact a *syenachiti* measuring 24 m × 18 m east-west direction and bears the shape of an eagle or hawk (the *Garuda* according to Hindu mythology). Various sizes of burnt bricks are reported for the construction of the *syenachiti*, ranging from 80 cm × 50 cm × 11 cm to 50 cm × 50 cm × 11 cm or even smaller. In the present study a small, burnt brick sample measuring 28 cm × 19 cm × 12.5 cm and approximating to half the size of the burnt clay brick (or block in present-day terminology) as used in the construction, was subjected to physical and

*For correspondence. (e-mail: jmb47in@yahoo.com)